



Preparation of gold nanopowders and nanoparticles using chitosan suspensions

Chao-Ming Shih^a, Yeong-Tarn Shieh^b, Yawo-Kuo Twu^{a,*}

^a Department of Bioindustry Technology, Dayeh University, Dacun, Changhua 51591, Taiwan, ROC

^b Department of Chemical and Materials Engineering, National University of Kaohsiung, Kaohsiung 81148, Taiwan, ROC

ARTICLE INFO

Article history:

Received 19 January 2009

Received in revised form 29 March 2009

Accepted 9 April 2009

Available online 22 April 2009

Keywords:

Chitosan

Nanopowder

Nanoparticle

Pyrolysis

Hydrolysis

ABSTRACT

Simple methods for preparation of gold nanopowders and nanoparticles are reported. Gold/chitosan nanoparticles were prepared by using basic chitosan suspension as a dispersant and as a reductant. The resulting nanoparticles were processed by pyrolysis and thus obtain black gold nanopowder. The FESEM images indicate that most diameters of the nanopowder prepared were in the range of 50 and 200 nm. Hydrolysis is another quick decomposition method for chitosan. Acetic acid was adopted to implement the hydrolysis. The AEM images of the auberginic suspension show that the average gold nanoparticle diameter was less than 40 nm with good dispersion. Use of chitosan suspensions can produce gold nanopowder as well as gold nanoparticle without using toxic organic chemicals.

© 2009 Elsevier Ltd. All rights reserved.

1. Introduction

Research on gold nanoparticles has been given much attention recently. The physicochemical property of gold is changed after it is processed through nanotechnology, and its derivative applications include the catalysis (Thompson, 2007), DNA sequence recognition (Eaton, Doria, Pereira, Baptista, & Franco, 2007), drug delivery (Oh et al., 2008), and electrochemical applications (Guo & Wang, 2007). Gold nanoparticles can be produced by means of laser ablation (Ko et al., 2006) and inert gas condensation (Lee, Park, & Lee, 2005). The advantage of these methods is that they can produce gold nanoparticles with narrow particle size distribution, but the shortcoming is the need for expensive equipment. Additionally, emulsification can also produce gold nanoparticles but with a wide distribution of particle diameters (Pal, Shah, & Devi, 2007). Gold nanocomposites are manufactured by using a reductant to reduce the gold ions and a dispersant in order to avoid excessive gold agglomeration. A unique shape of gold nanoboxes and silver nanocubes can be achieved by self-assembly through Sun and Xia's utilization of poly(vinyl pyrrolidone) as a dispersing agent (Sun & Xia, 2002). When sodium borohydride is taken as the reductant, the dispersants used in the preparation of gold nanocomposites are poly(amidoamine) dendrimers, poly-(propyleneimine) dendrimers (Esumi, Miyamoto, & Yoshimura, 2002),

horse spleen apoferritin (Zhang, Swift, Butts, Yerubandi, & Dmochowski, 2007), and tryptophan (Selvakannan et al., 2004). Meanwhile, when sodium citrate is taken as the reductant, the dispersants used are 1- α -dipalmitoyl-phosphatidylcholine (Zhu, Tao, Zheng, & Li, 2005), 1,4,7,10,13,16,21,24-octaaza-bicyclo [8.8.8]hexacosane (azacryptand) (Lee, Hwang, Lee, Kim, & Han, 2007). The alkylamine-stabilized gold nanocomposite is prepared by using ethanol reduction through microwave irradiation (Shen, Du, Hua, & Yang, 2006). Some of the above manufacturing processes cause harm to the environment due to the toxic chemicals used.

Chitosan, a *N*-deacetylation product of chitin, which is a non-toxic biopolymer was applied on the reclamation of metal cations, such as Mg^{2+} , Cr^{3+} , Fe^{2+} , Co^{2+} , Ni^{2+} , Cu^{2+} , Zn^{2+} , Cd^{2+} , Hg^{2+} , and Pb^{2+} (Assaad et al., 2007; Gamage & Shahidi, 2007; Vasconcelos et al., 2008; Yang, Li, Chou, & Chou, 2005; Yang, Shu, Zhang, & Wang, 2006), where chelates of chitosan molecules and metal cations are precipitated. Relevant theses have been found about the utilization of chitosan and its effects on the preparation of precious metal (Pd, Ag, Pt, and Au) nanocomposites (Adlim, Bakar, Liew, & Ismail, 2004; Arrascue, Garcia, Horna, & Guibal, 2003; Esumi, Takei, & Yoshimura, 2003; Huang & Yang, 2003; Huang, Yuan, & Yang, 2004, 2005), in which chitosan acts as the dispersant to avoid the occurrence of metal particles agglomeration. In our previous report, silver nanoparticles were prepared by using alkaline chitosan suspension as a dispersant and as a reductant in the absence of other chemicals. Silver nanoparticles were obtained by annealing silver/chitosan composites (Twu, Chen, & Shih, 2008). In this study, utilization of chitosan suspensions to manufacture gold nanopowders and nanoparticles by means of pyrolysis and acid hydrolysis is described.

* Corresponding author. Address: Department of Bioindustry Technology, Dayeh University, 112 Shanjiao Rd., Dacun, Changhua 51591, Taiwan, ROC. Tel.: +886 4 8511319.

E-mail address: poly2001@mail.dyu.edu.tw (Y.-K. Twu).

2. Experimental method

2.1. Materials and methods

Chitosan ($M_v = 750$ kDa, degree of deacetylation = 85%) was obtained from QBAS Co. The chitosan solution (1%) was prepared by dissolving 5 g of chitosan in 500 mL of 0.12 M CH_3COOH solution. A stock gold solution was prepared by mixing 1 g gold (99.99% pure) and 20 mL royal water. Royal water was prepared by freshly mixing concentrated nitric acid and concentrated hydrochloric acid in a volumetric ratio of 1:3, respectively. Concentrated HCl, HNO_3 and all other chemicals were used as received. The water used in this experiment was purified by a double deionization of reverse osmosis water. UV–vis absorbance spectra were collected by a JASCO V-530 double-beam spectrophotometer. A distinct absorption was observed at about 530 nm which is the characteristic plasmon absorption peak of gold nanoparticles (Huang et al., 2005). Analytical electron microscopic (AEM) micrographs and selected area electron diffraction (SAED) data were acquired with a JEOL JEM-1200CX II electron microscope operating at 120 kV. Samples for the AEM were prepared by placing a drop of Au/chitosan suspension onto a carbon-coated copper grid and evaporating the water in a laboratory hood at room temperature. The surface morphology of the Au nanopowders and nanoparticles was observed by a JEOL JSM-6700F field emission scanning electron microscope (FESEM). The elemental analysis of the particles was identified by the FESEM equipped with an OXFORD INCA ENERGY 400 energy dispersive X-ray spectrum (EDS). The size distributions of the Au/chitosan and Au nanoparticles were measured from the enlarged AEM and FESEM micrographs, respectively, by counting at least 200 individual particles from different regions on a film.

2.2. Preparation of gold/chitosan suspensions

A milk-like alkaline chitosan suspension with $\text{pH} > 14$ was produced after using 500 mL 1% (w/v) of chitosan acetic acid solution, dripping it into a 500 mL sodium hydroxide solution of 3.6 N, and mixing them together with a homogenizer (Art MICCRA D-8, Germany) at 10,500 rpm. To evaluate the effect of chitosan content in the alkaline suspension on the formation of gold nanoparticles, the molar ratio of the gold to the chitosan repeating units was set to 1:1, 1:3, and 1:5, respectively. To the chitosan suspensions

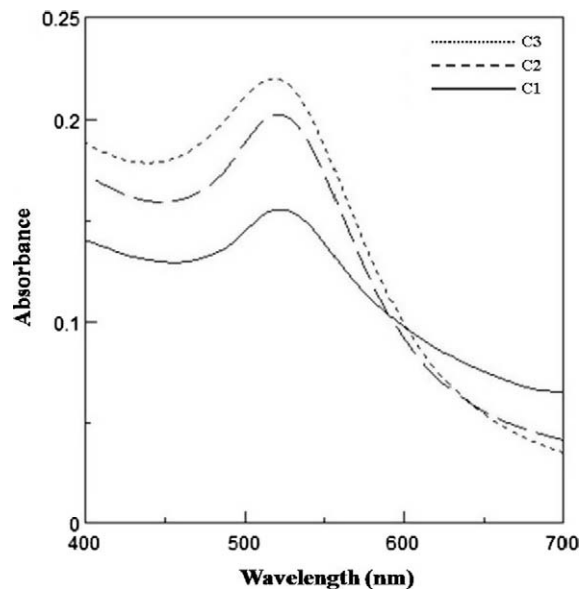


Fig. 2. UV–vis spectra recorded from C1, C2 and C3, 16 h after reaction.

of 42.6, 127.8, and 213.0 mL, deionized water was added, respectively, and their volume was adjusted to 245 mL. Then 5 mL of gold solution was taken and dripped into each suspension under homogenization. The pH of the complex suspension was 12.6, 13.3, and 13.5, respectively. Subsequently, it was stirred under room temperature with a magnetic stirrer for 16 h, during which 4 mL of the suspension was removed at 0 h, 0.5 h, 1 h, 4 h, and 16 h, respectively; this was followed by scanning its absorption with UV–vis. Finally, purple neutral suspensions were produced when rinsing the alkaline suspensions with deionized water repeatedly after 16 h. At the same time, the products were marked as C1, C2, and C3, respectively, and then examined with AEM.

2.3. Preparation of gold nanopowders by pyrolysis

The process began with 5 drops of C1, C2, and C3 added to the Ag holder (5 mm \times 5 mm). After removing the moisture by heating at 80 $^{\circ}\text{C}$, the temperature of the sample was increased to 600 $^{\circ}\text{C}$ for

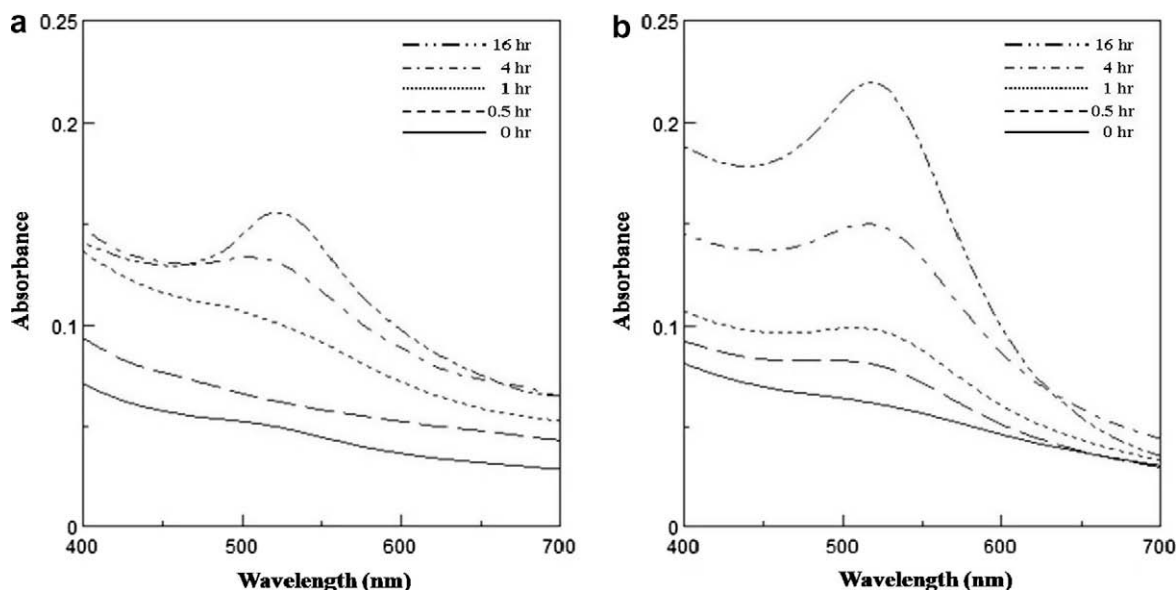


Fig. 1. UV–vis spectra of basic Au/chitosan suspensions (a) C1 and (b) C3.

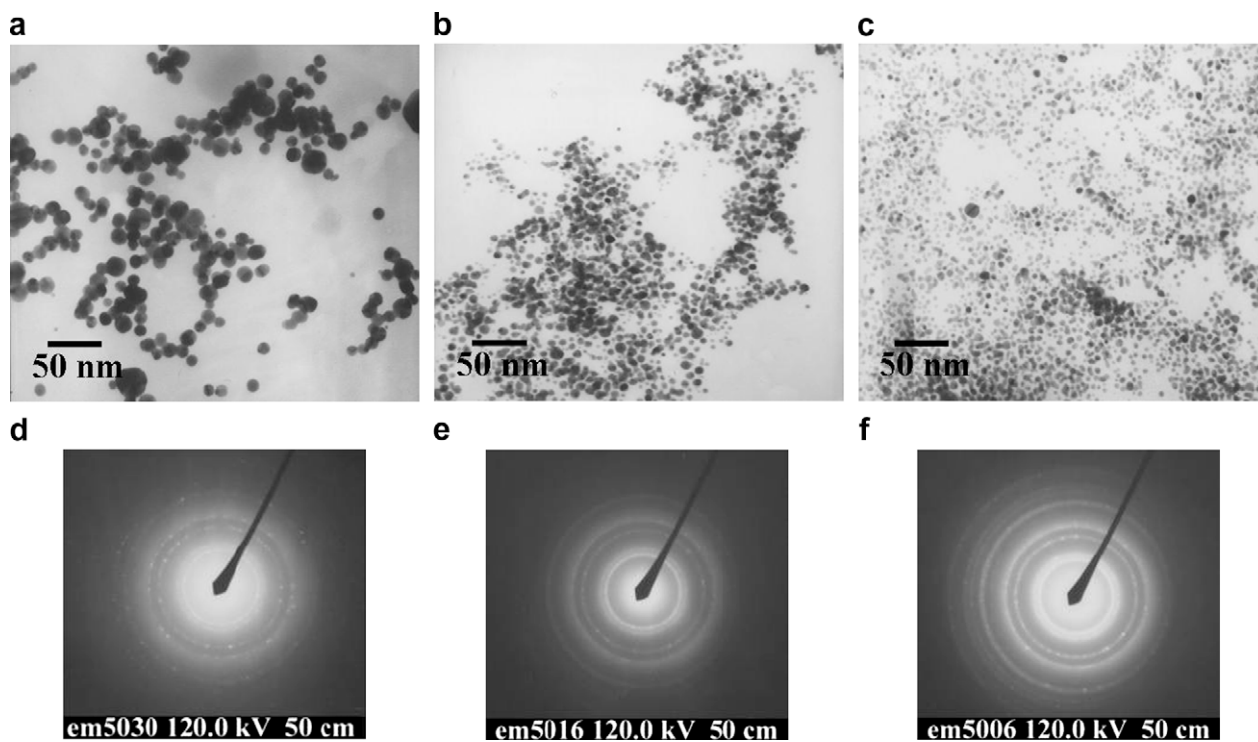


Fig. 3. AEM images of (a) C1; (b) C2; and (c) C3, and their SAED patterns (d); (e); and (f) from selected areas of samples, respectively.

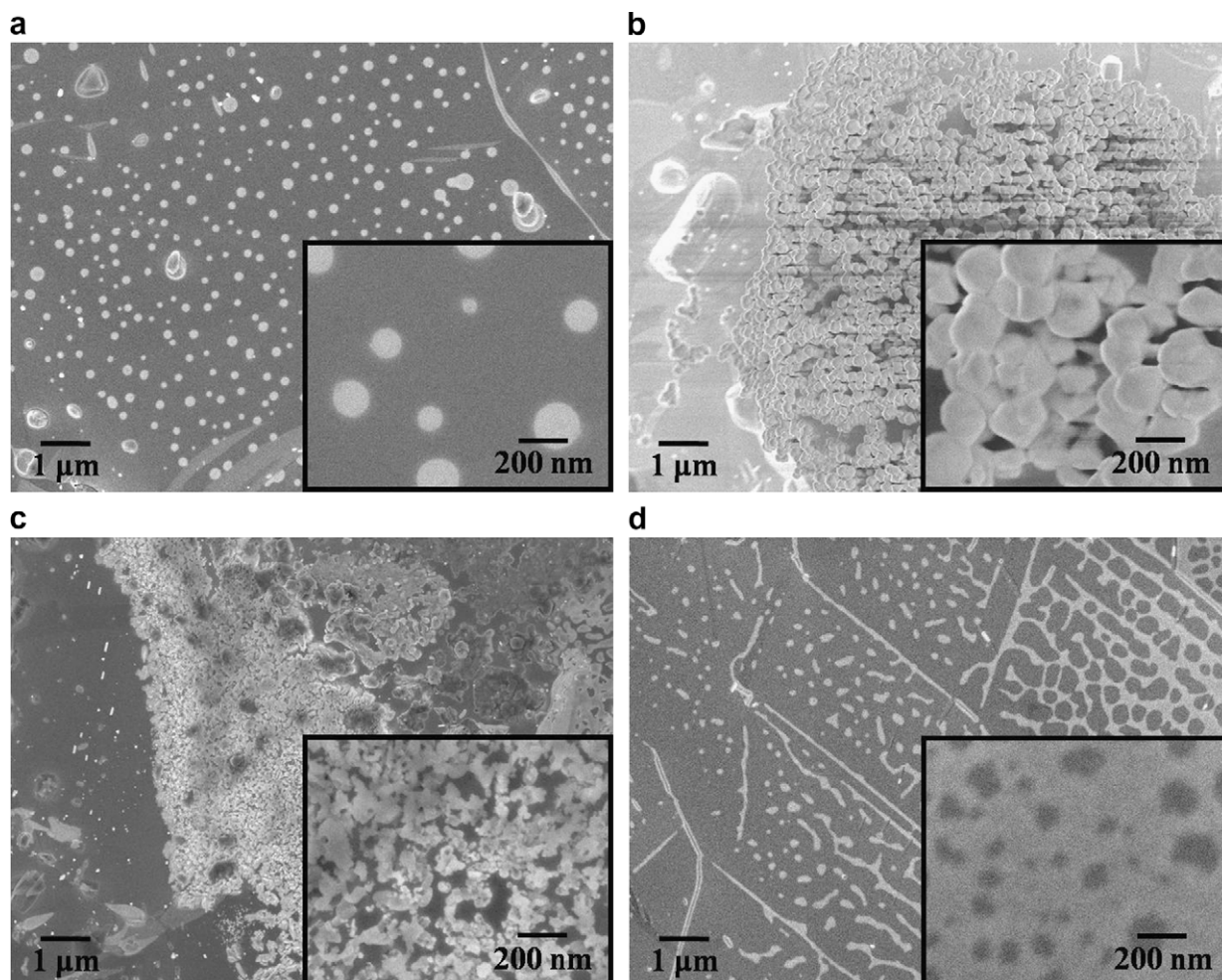


Fig. 4. FESEM images of (a) C1/600; (b) C1/800; (c) C3/600; and (d) C3/800 recorded from as-prepared Au nanostructures on Ag holder obtained by pyrolysis, and their enlarged images.

1 h at a speed of 20 °C/min using a horizontal tube furnace and quartz tube reactor (Shang-Mei, CWF) in air. Black powders were then obtained and labeled as C1/600, C2/600, and C3/600, respectively, after they were cooled by nitrogen. With the same process but heating up to 800 °C, another set of black powders was produced and labeled as C1/800, C2/800, and C3/800. Each sample was examined by FESEM and EDS.

2.4. Preparation of gold nanoparticles by hydrolysis

After 50 mL of C1, C2, and C3, respectively, were centrifuged at a speed of 17,000 rpm for 60 min, the sediments were put into acetic acid solutions (500 mL, 3 M) and subjected to hydrolysis for 1 h at 100 °C. They were then centrifuged at a speed of 17,000 rpm for 30 min. Their auberginic supernatant was taken and labeled as C1H1, C2H1, and C3H1, and then examined with AEM. The traces of the centrifuged sediments were labeled as C1H2, C2H2, and C3H2, respectively, and were examined with FES-EM and EDS.

3. Results and discussion

3.1. Reduction of gold ions

In preliminary studies, no transparent or color variation occurred in the intermixture of gold solution mixed with a chitosan acidic solution. At the same time, no distinct absorption peak of gold nanoparticles occurred on the UV–vis spectra. According to the literatures (Esumi et al., 2003; Huang et al., 2005), the distinct absorption peak from the surface plasmon absorption of the gold nanoparticles is located between 510 and 530 nm. The UV–vis spectra proved that the gold ions cannot be reduced by the chitosan acidic solution. We previously reported that the chitosan alkaline suspension has the capacity to reduce silver ions. The

dispersed Ag^+ /chitosan produced by the chelation of silver ion and chitosan can acquire an electron in alkaline conditions and then can be reduced into Ag/chitosan nanoparticles (Twu et al., 2008).

In this study, the suspension of the gold solution mixed with the chitosan alkaline suspension turned grey immediately. The color also changed gradually into purple in the reaction. Fig. 1a and b show the results observed by UV–vis during the alkaline suspension reaction of C1 and C3, respectively. From Fig. 1, it can be seen that an absorption peak at about 520 nm occurs, and that its strength increases as time elapses. From this, we can infer that gold ion was reduced in the suspension. After reacting for 1 h, the absorption peak occurs in C1, while C3 needs only 0.5 h. Therefore, a higher reduction rate was observed in C3 suspension than in C1, and that there was a higher amount of reducing groups in C3 suspension provided for gold ion's reduction in a condition with greater alkalinity. The reason for the chitosan alkaline suspension's capability of reducing the gold ion may be a result of the low molecular weight oligosaccharide from chitosan decomposing in an alkaline condition, which provides the electron for reduction (Sun et al., 2008).

To evaluate the effect of chitosan content in the alkaline suspension on the formation of gold nanoparticles, the molar ratio of the gold ion to the chitosan repeating units was set to 1:1, 1:3, and 1:5, respectively, in the starting suspension of C1, C2, and C3. Fig. 2 indicates UV–vis spectra recorded from various formulas 16 h after the reaction. The positions of their absorption peaks are C1 (522 nm), C2 (521 nm), and C3 (518 nm), respectively. Newman (Newman, Roberts, & Blanchard, 2007) demonstrated that the gold distinct absorption peak caused a red shift as the gold particle diameter increased. From the blue shifts of various absorption peaks as the content of chitosan increased in Fig. 2, we can infer that the diameters of various sample particles decreased as the content of chitosan increased.

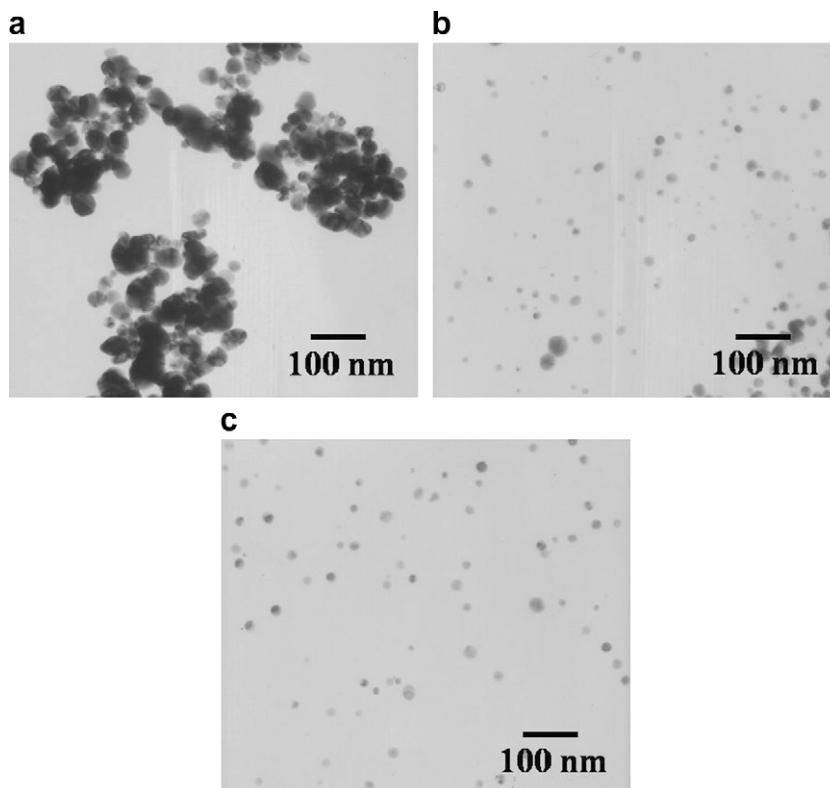


Fig. 5. AEM images of Au nanoparticles (a) C1H1; (b) C2H1; and (c) C3H1.

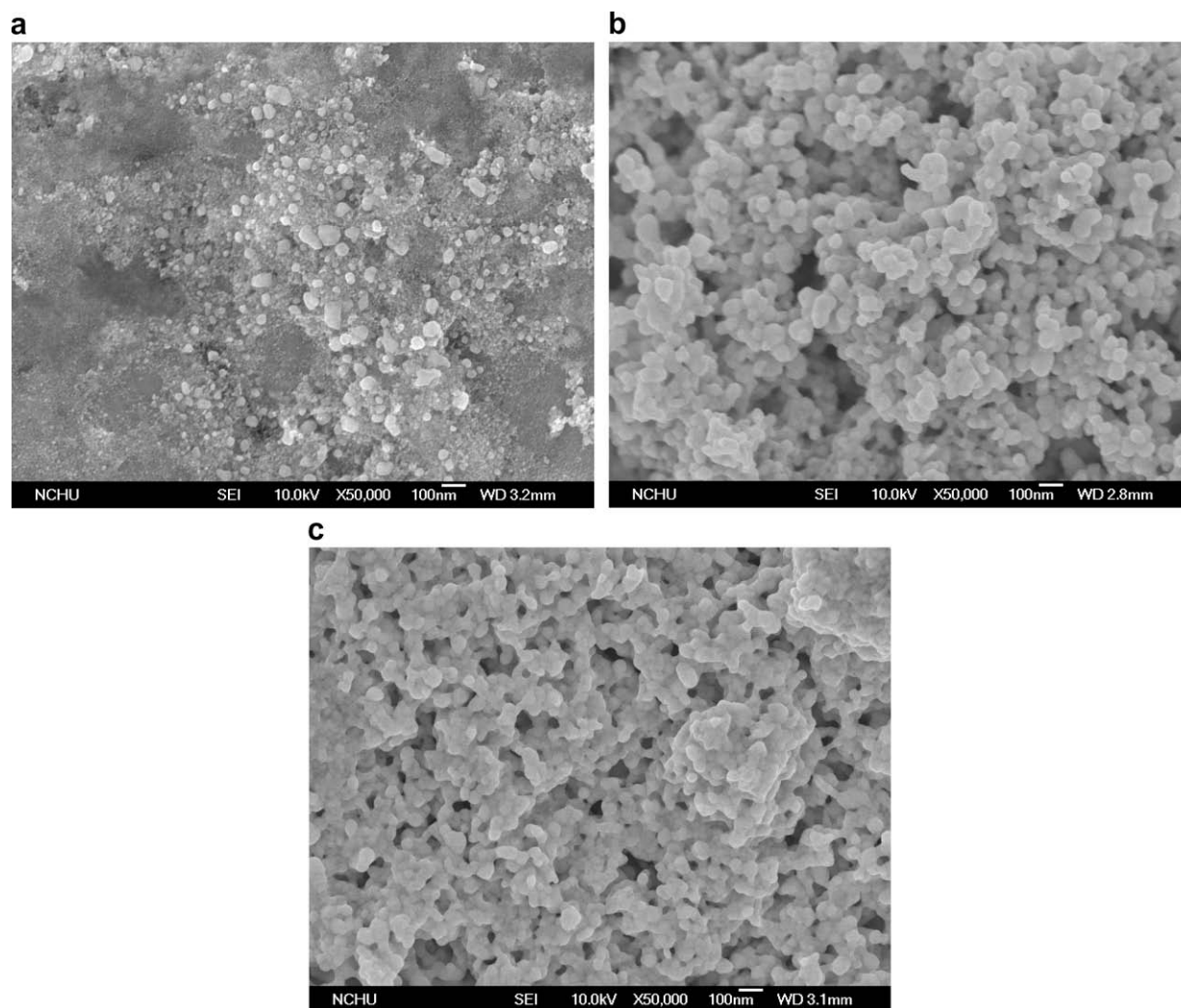


Fig. 6. FESEM images of Au nanoparticles (a) C1H2; (b) C2H2; and (c) C3H2.

3.2. Au/chitosan suspensions

Fig. 3a, b, and c show the analysis results for C1, C2, and C3 after AEM and SAED analysis. Each sample was granular pellets with average particle diameters of 35 ± 4.7 nm, 20 ± 3.4 nm, and 15 ± 2.1 nm, respectively, which conforms to the inference made from Fig. 2. The comparison on particle diameters proves that gold ions can disperse evenly in a suspension with higher chitosan content. When the gold ions are reduced into gold atoms, this can prevent the gold atoms from gathering and coagulating with excessively large diameters.

In addition, the rate of gold ion reduction rapidly increased, which in turn decreased the chance for the gold atom to gather into large particles as the pH value increased. Analysis of SAED in Fig. 3a indicates that there are obvious spots on the SAED image of C1, each spot corresponding to a satisfied diffraction condition of the gold's crystalline structure. This also implies that the C1 particles have a more integral crystal structure of gold. A diffused halo can verify the amorphous structure of chitosan. However, the scattered spots of SAED in Fig. 3b and c are not obvious, which indicates that the degree of crystallization of the C2 and C3 gold particles were more inferior. As the content of chitosan increased along with the various formulas, its disaggregation on the gold ion increased as well, that prevented the much bigger gold crystals from being produced during the gold ion reduction process. Analysis of AEM

and SAED has proven that chitosan can act as the dispersant in the suspension.

3.3. Au nanopowders prepared by pyrolysis

Fig. 4a and b show the FESEM images of the black powder of the C1 after pyrolysis at 600 °C and 800 °C, respectively. Fig. 4a indicates that most diameters of the gold particles are in the range of 50 and 200 nm, with only a few resulting in fusion. Fig. 4b shows that the diameters of the gold particles are more than 200 nm even with a serious fusion, which cannot be dispersed. The melting point of gold is 1064 °C, while the melting point of gold nanoparticle will be lowered as its diameter decreases (Liu, Ascencio, Perez-Alvarez, & Yacaman, 2001). The average particle diameter of the C1 was 35 nm in which the particle diameter of the embedded gold particles was less than this value. When C1/600 was made from 600 °C pyrolysis, chitosan were decomposed, and the remaining gold particles fused with the others around them to form particles with a diameter of more than 35 nm. At 800 °C pyrolysis, much bigger particles were produced, which cannot be dispersed. Fig. 4c and d are the FESEM images of the C3 after pyrolysis at 600 °C and 800 °C, respectively. As the average particle diameter of the C3 was only 15 nm, the embedded gold particles also have a diameter less than this value. When C3/600 was made from 600 °C pyrolysis, a large amount of chitosan was decomposed,

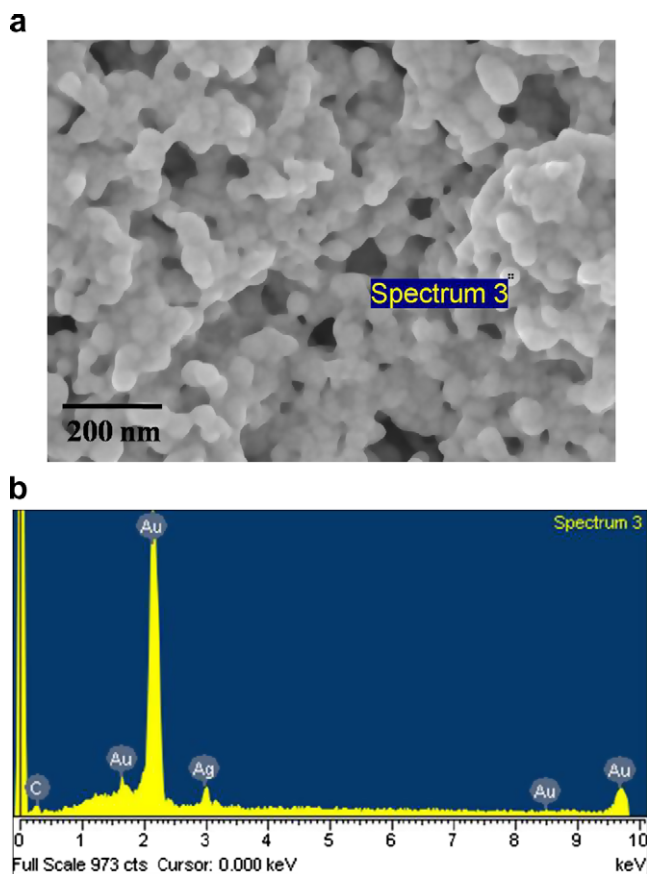


Fig. 7. Characterization of Au particles from C3H2 using (a) FESEM and (b) EDS from a selected area.

and the remaining gold particles were heated and fused with the others around them to form particles with irregular and dispersed gold particles. At 800 °C pyrolysis, an agglomerate structure with serial arrangement was produced, and at the same time, the particles would disappear and melt into a spotted, linear, or laminate structure.

The aim of pyrolysis is to decompose or eliminate the chitosan. However, if the temperature is lower than 600 °C, more pyrolysis time is needed. Previous results show that there are a much higher proportion of carbon atoms that remain on the silver holder through the FESEM and EDS analysis. When the sample undergoes 600 °C pyrolysis, the content of chitosan will directly influence the size of the gold particles as well as their melting point, which results in the fusion of a few smaller particles. At 800 °C pyrolysis, the melting of gold particles ensues, which is unsuitable for the preparation of gold nanopowder.

3.4. Au nanoparticles prepared by hydrolysis

Apart from thermal degradation, acid hydrolysis is another quick decomposition method for chitosan. When the Au/chitosan particle was dissolved in strong acid, such as hydrochloric acid, nitric acid and sulfuric acid, the oxidation of the gold atom will occur once again. Therefore, acetic acid was adopted in this study in order to implement the hydrolysis. Fig. 5a, b, and c show the AEM images of the auberginic supernatant fluid of C1H1, C2H1, and C3H1, respectively. The average particle diameters of C1H1, C2H1, and C3H1 were 37 ± 19.6 nm, 15 ± 6.5 nm, and 14 ± 4.1 nm, respectively, which were similar to that of the un-hydrolyzed one. This indicates that the gold particles can be released directly from the composite particles without agglomeration. Fig. 6a, b,

and c show the FESEM images of the black sediments of C1H2, C2H2, and C3H2, respectively. Centrifugation often results in aggregates and agglomerates rather than singleton primary particles. The size of primary gold particles increased insignificantly. However, a porous secondary nanostructure was formed among the particles because of the increasing collision of the gold particles in centrifugation. This was clear in C2H2 and C3H2 and more so for C3H2 than C2H2.

The observation of the hydrolysis and the comparison between Figs. 5 and 6 indicates that under the same hydrolysis conditions, the C1 sample with a lower content of chitosan can release gold particles more quickly and produce a deeper color of suspension but with a lowest yield of black sediment. With the high chitosan content of C2 and C3, hydrolysis cannot release the gold particles immediately. This resulted in the mass gathering of the gold particles, with fewer gold particles released, as well as the light color of the supernatant with a higher yield of black sediment.

Fig. 7 depict the EDS analysis from a selected area of C3H2. The EDS quantitative analysis confirmed that the gold content has the highest elementary composition, while silver has a minor content together with only a trace of carbon. Thus, the silver signal came from the silver holder, while the carbon signal was from the incompletely hydrolyzed chitosan. FESEM and EDS have proven that porous gold nanostructure was produced through hydrolysis on Au/chitosan suspension.

4. Conclusions

This paper reports simple methods for the preparation of gold nanopowders and nanoparticles by using basic chitosan suspension as a dispersant and a reductant. Gold/chitosan suspensions were prepared and followed by treatment with the pyrolysis in order to decompose the chitosan from the gold/chitosan and to obtain gold nanopowders. When gold/chitosan underwent 600 °C pyrolysis, the content of chitosan directly influenced the size of the gold particles as well as their melting point, which resulted in the fusion of a few smaller particles. At 800 °C pyrolysis, an agglomerate structure with serial arrangement was produced, and at the same time, the particle disappeared and melted into a spotted, linear, or laminate structure.

Hydrolysis was another quick decomposition method for chitosan. The gold/chitosan was put into acetic acid solutions and underwent hydrolysis and then was centrifuged. Analysis of the auberginic supernatant data indicated that the gold nanoparticles can be released directly from gold/chitosan without agglomeration. However, the centrifuged sediments were found to have not only an increased size of specific gold particles but to have formed a porous nanostructure among the particles with the increasing collision in the gold particles in centrifugalization.

Acknowledgements

This research was financially supported by Grant No. NSC-93-2313-B-212-004 from the National Science Council of the Republic of China. FESEM and AEM assistance from Regional Instruments Center, National Chung Hsing University, is gratefully acknowledged.

References

- Adlim, M., Bakar, M. A., Liew, K. Y., & Ismail, J. (2004). Synthesis of chitosan-stabilized platinum and palladium nanoparticles and their hydrogenation activity. *Journal of Molecular Catalysis A: Chemical*, 212, 141–149.
- Arrascue, M. L., Garcia, H. M., Horna, O., & Guibal, E. (2003). Gold sorption on chitosan derivatives. *Hydrometallurgy*, 71, 191–200.
- Assaad, E., Azzouz, A., Nistor, D., Ursu, A. V., Sajin, T., Miron, D. N., et al. (2007). Metal removal through synergic coagulation–flocculation using an optimized chitosan–montmorillonite system. *Applied Clay Science*, 37, 258–274.

- Eaton, P., Doria, G., Pereira, E., Baptista, P. V., & Franco, R. (2007). Imaging gold nanoparticles for DNA sequence recognition in biomedical applications. *IEEE Transactions on Nanobioscience*, 6(4), 282–288.
- Esumi, K., Takei, N., & Yoshimura, T. (2003). Antioxidant-potentiality of gold–chitosan nanocomposites. *Colloid Surfaces B: Biointerfaces*, 32, 117–123.
- Esumi, K., Miyamoto, K., & Yoshimura, T. (2002). Comparison of PAMAM–Au and PPI–Au nanocomposites and their catalytic activity for reduction of 4-nitrophenol. *Journal of Colloid Interface Science*, 254, 402–405.
- Gamage, A., & Shahidi, F. (2007). Use of chitosan for the removal of metal ion contaminants and proteins from water. *Food Chemistry*, 104, 989–996.
- Guo, S., & Wang, E. (2007). Synthesis and electrochemical applications of gold nanoparticles. *Analytica Chimica Acta*, 598, 181–192.
- Huang, H., Yuan, Q., & Yang, X. (2005). Morphology study of gold–chitosan nanocomposites. *Journal of Colloid Interface Science*, 282, 26–31.
- Huang, H., Yuan, Q., & Yang, X. (2004). Preparation and characterization of metal–chitosan nanocomposites. *Colloid and Surface B: Biointerfaces*, 39, 31–37.
- Huang, H., & Yang, X. (2003). Chitosan mediated assembly of gold nanoparticles multilayer. *Colloid and Surface A: Physicochemical and Engineering Aspects*, 226, 77–86.
- Ko, S. H., Choi, Y., Hwang, D. J., Grigoropoulos, C. P., Chung, J., & Poulikakos, D. (2006). Nanosecond laser ablation of gold nanoparticle films. *Applied Physics Letters*, 89, 141126.
- Lee, K. M., Park, S. T., & Lee, D. J. (2005). Nanogold synthesis by inert gas condensation for immuno-chemistry probes. *Journal of Alloys and Compounds*, 390, 297–300.
- Lee, K. Y., Hwang, J., Lee, Y. W., Kim, J., & Han, S. W. (2007). One-step synthesis of gold nanoparticles using azacryptand and their applications in SERS and catalysis. *Journal of Colloid Interface Science*, 316, 476–481.
- Liu, H. B., Ascencio, J. A., Perez-Alvarez, M., & Yacaman, M. J. (2001). Melting behavior of nanometer sized gold isomers. *Surface Science*, 491, 88–98.
- Newman, J. D. S., Roberts, J. M., & Blanchard, G. J. (2007). Optical organo-phosphate/phosphonate sensor based upon gold nanoparticle functionalized quartz. *Analytica Chimica Acta*, 602, 101–107.
- Oh, K. S., Kim, R. S., Lee, J., Kim, D., Cho, S. H., & Yuk, S. H. (2008). Gold/chitosan/pluronic composite nanoparticles for drug delivery. *Journal of Applied Polymer Science*, 108, 3239–3244.
- Pal, A., Shah, S., & Devi, S. (2007). Preparation of silver, gold and silver–gold bimetallic nanoparticles in w/o microemulsion containing Triton X-100. *Colloids and Surface A: Physicochemical and Engineering Aspects*, 302, 483–487.
- Selvakannan, P. R., Mandal, S., Phadtare, S., Gole, A., Pasricha, R., Adyanthaya, S. D., et al. (2004). Water-dispersible tryptophan-protected gold nanoparticles prepared by the spontaneous reduction of aqueous chloroaurate ions by the amino acid. *Journal of Colloid and Interface Science*, 269, 97–102.
- Shen, M., Du, Y., Hua, N., & Yang, P. (2006). Microwave irradiation synthesis and self-assembly of alkylamine-stabilized gold nanoparticles. *Powder Technology*, 162, 64–72.
- Sun, C., Qu, R., Chen, H., Ji, C., Wang, C., Sun, Y., et al. (2008). Degradation behavior of chitosan in the “green” synthesis of gold nanoparticles. *Carbohydrate Research*, 343, 2595–2599.
- Sun, Y., & Xia, Y. (2002). Shape-controlled synthesis of gold and silver nanoparticles. *Science*, 298(5601), 2176–2179.
- Thompson, D. T. (2007). Using gold nanoparticles for catalysis. *Nanotoday*, 2(4), 40–43.
- Twu, Y. K., Chen, Y. W., & Shih, C. M. (2008). Preparation of silver nanoparticles using chitosan suspensions. *Powder Technology*, 185, 251–257.
- Vasconcelos, H. L., Camargo, T. P., Gonçalves, N. S., Neves, A., Laranjeira, M. C. M., & Fávere, V. T. (2008). Chitosan crosslinked with a metal complexing agent: Synthesis, characterization and copper(II) ions adsorption. *Reactive Functional Polymers*, 68, 572–579.
- Yang, T. C., Li, C. F., Chou, S. S., & Chou, C. C. (2005). Adsorption of metal cations by water-soluble N-alkylated disaccharide chitosan derivatives. *Journal of Applied Polymer Science*, 98, 564–570.
- Yang, Z., Shu, J., Zhang, L., & Wang, Y. (2006). Preparation and adsorption behavior for metal ions of cyclic polyamine derivative of chitosan. *Journal of Applied Polymer Science*, 100, 3018–3023.
- Zhang, L., Swift, J., Butts, C. A., Yerubandi, V., & Dmochowski, I. J. (2007). Structure and activity of apoferritin-stabilized gold nanoparticles. *Journal Inorganic Biochemistry*, 101, 1719–1729.
- Zhu, H., Tao, C., Zheng, S., & Li, J. (2005). One step synthesis and phase transition of phospholipid-modified Au particles into toluene. *Colloids and Surfaces A: Physicochemical and Engineering Aspects*, 257–258, 411–414.